

Article

Performance of Al₂O₃/TiO₂ Hybrid Nano-Cutting Fluid in MQL Turning Operation via RSM Approach

Ariffin Arifuddin ¹, Abd Aziz Mohammad Redhwan ¹, Wan Hamzah Azmi ^{2,3,*} and Nurul Nadia Mohd Zawawi ² ¹ Faculty of Engineering Technology, University College TATI, Kemaman 24000, Terengganu, Malaysia² Centre for Research in Advanced Fluid and Processes, Lebuhraya Tun Razak, Gambang, Kuantan 26300, Pahang, Malaysia³ Faculty of Mechanical and Automotive Engineering Technology, Universiti Malaysia Pahang, Pekan 26600, Pahang, Malaysia

* Correspondence: wanazmi@ump.edu.my; Tel.: +60-9-4246338 or +60-9-4242202

Abstract: Cutting fluids can be used to cool workpieces at high cutting speeds and remove chips from cutting zones. The effectiveness of cutting fluids may be improved with the addition of hybrid nanoparticle dispersion. This study evaluates the effectiveness of an Al₂O₃-TiO₂ hybrid as a cutting fluid in turning operations. The Al₂O₃-TiO₂ hybrid nano-cutting fluid was prepared using a one-step method in computer numerical control (CNC) coolant with concentrations of up to 4%. Utilizing air-assisted nano-cutting fluids injected through a minimum quantity lubrication (MQL) setup, the effectiveness of turning cutting performance, cutting temperature (°C), average surface roughness (Ra), and tool wear (%) were evaluated. Then, the response surface method (RSM) was utilized as the design of experiment (DOE) to optimize the turning cutting performance parameters. The combination of 4% hybrid nano-cutting fluid concentration, 0.1 mm/rev feed rate, and 0.55 mm depth of cut yielded the lowest cutting temperature, surface roughness, and tool wear values of 25.3 °C, 0.480 μm, and 0.0104%, respectively. The 4% concentration of Al₂O₃/TiO₂ hybrid nano-cutting fluid inclusion achieved the highest surface roughness reduction that led to better surface finish and the lowest tool-wear reduction led to longer tool life. Therefore, Al₂O₃/TiO₂ hybrid nano-cutting fluids were strongly recommended in turning operations for CNC lathes.

Keywords: minimum quantity lubrication; Al₂O₃-TiO₂ hybrid nanofluids; nano-cutting fluid; CNC turning; response surface method



Citation: Arifuddin, A.; Redhwan, A.A.M.; Azmi, W.H.; Zawawi, N.N.M. Performance of Al₂O₃/TiO₂ Hybrid Nano-Cutting Fluid in MQL Turning Operation via RSM Approach. *Lubricants* **2022**, *10*, 366. <https://doi.org/10.3390/lubricants10120366>

Received: 23 November 2022

Accepted: 14 December 2022

Published: 16 December 2022

Publisher's Note: MDPI stays neutral with regard to jurisdictional claims in published maps and institutional affiliations.



Copyright: © 2022 by the authors. Licensee MDPI, Basel, Switzerland. This article is an open access article distributed under the terms and conditions of the Creative Commons Attribution (CC BY) license (<https://creativecommons.org/licenses/by/4.0/>).

1. Introduction

Machining is an essential step in the manufacturing process. The manufacturing industry, in which desired components and parts are obtained by removing material in the form of chips, is the industry in which it possesses the greatest degree of versatility. The friction between the tool and the workpiece during any machining generates significant heat at the machining zone. The requisite surface quality and tool life cannot be achieved in dry machining due to the excessive heat generation at the cutting zone, which affects the hardness and sharpness of the cutting tool. The higher the temperature, the greater the risk that the cutting tool will fail prematurely, and the surface quality of the workpiece will be inferior [1,2]. During cutting in machining, common cooling procedures include the dry technique, the flood technique, and the minimum-quantity lubrication (MQL) technique. These cooling techniques are used to reduce wear during the cutting process, prolong tool life, and reduce the temperature of the cutting process. The dry technique is limited by its propensity to create high temperatures, which induces excessive tool wear, and the tendency of formed chips to tangle at the tool tip and in the cutting zone, which can reduce tool life and provide a poor surface quality [3]. Meanwhile, the current flood approach minimises working temperature and tool wear while enhancing the quality of the surface finish. However, the excessive use of coolant in flood techniques results in environmental

and health concerns. Consequently, the MQL approach, which utilizes a very little amount of cutting fluids, is a viable alternative for eliminating the limitations of both the dry and flood cutting methods.

The use of MQL, which minimizes coolant consumption and costs while offering the greatest level of environmental protection, has recently attracted the attention of researchers. According to Sharma et al. [4], there is a negligible difference in cutting performance between MQL and flood machining utilizing standard cutting fluid. Unlike flood lubrication, MQL requires only a few milliliters (ml) of lubricant per hour for the machining operation. In their investigation, Shao et al. [5] shown that the technique was comparable to flood-cooling grinding in terms of surface quality, grinding force, and residual stresses, while drastically reducing lubricant costs. Moreover, compared to dry circumstances, the grinding temperature was greatly reduced. Mulyadi et al. [6] evaluated the tool life of H13 tool steel under the conditions of MQL, dry machining, and flood machining. The H13 cutting tool steel is a type of chromium-molybdenum hot work steel. It is renowned for its excellent resistance to heat and abrasion. Consequently, it is suited for a variety of hot work applications, such as cutting tools. The researchers concluded from their observations that the MQL can reduce machining costs and environmental issues by lowering cutting fluid usage. As a continuation of their work, the researchers have investigated the possibility of combining MQL with nanoparticles to further improve the method's effectiveness.

The stability of the nano-cutting fluid is one of the characteristics that must be examined to achieve maximum or optimal machining performance, and current research is focused on developing a better and more complex cutting fluid, which is nano-cutting fluid for turning machine machining. Moreover, the influence of particle concentration on the stability of water-based nanofluids must be addressed [7]. The nano-cutting fluid is designed to suit the increasing cooling and lubrication demands of the machining industry. Nevertheless, relatively little study on nano-cutting fluid has been conducted up to this point. Sharma et al. [8] implemented the usage of nanoparticles in the MQL turning process. For turning AISI 1040 steel, nano-cutting fluid was created by adding 1 vol. % of Al_2O_3 to vegetable oil and 5 vol. % of oil to a water emulsion. Compared to wet or flood machining, the surface roughness, tool wear, and cutting force were reduced by up to 25.5%, 5.27%, and 28%, respectively. Few researchers have attempted to integrate or combine more than two nanofluid types to create hybrid nanofluids. Hybrid nanofluids are described as the combining of two or more nanoparticles to produce hybrid nanofluids; this type of nanofluid is anticipated to outperform single nanoparticle performance. Singh et al. [9] evaluated the performance of an Al_2O_3 -graphene hybrid cutting fluid in hard turning. The study revealed that Al_2O_3 -graphene blending enhances the performance of hybrid nano-cutting fluids. Meanwhile, hybrid nano-cutting fluid and MQL significantly reduce surface roughness by 20.28% and cutting force, thrust force, and feed force by 9.94%, 17.38%, and 7.25%, respectively, compared to coolant as the base fluid. Numerous researchers have made attempts to incorporate various nanoparticle types into cutting fluids, but none of them have included both Al_2O_3 and TiO_2 nanoparticles. However, research on the hybrid nano application of MQL cooling technology for turning is still insufficient.

Cutting performance parameters such as cutting temperature [10], surface roughness [11], and tool wear [12] are improved during the turning process using hybrid nano-cutting fluid via the MQL cooling technique. DOE approaches such as factorial design, response surface methodology, and Taguchi methods have largely replaced the time-consuming and expensive one-factor-at-a-time experimental approach [13]. To find the optimal performance parameters for generating more effective and environmentally friendly machinability conditions of the materials, more exhaustive research must be conducted. Adjusting the parameters that influence the cutting performance of the machining system may be carried out quantitatively and on a regular basis with the assistance of the response surface methodology (RSM), which can help achieve optimal performance. The RSM optimization technique has been employed in a few studies to identify the ideal operating parameters for systems utilizing nanofluids.

Thus, the purpose of this research is to explore the optimum performance of an Al_2O_3 - TiO_2 hybrid nano-cutting fluid in turning applications with the aid of the MQL cooling technique. Therefore, in this investigation, the Al_2O_3 - TiO_2 hybrid nanofluid was produced by a one-step method preparation. A qualitative data observation, such as visual sedimentation, and a quantitative data observation, such as analysis using a UV-Vis photometer and zeta potential, were both utilized in order to evaluate the stability of the nanofluid. Then, using the RSM, an optimal performance study for the turning machine's machining process was performed.

2. Materials and Methods

2.1. Materials and Properties of Hybrid Nanofluid

Metal oxide nanoparticles made of Al_2O_3 and TiO_2 in liquid solution with nanoparticles inside were used in this investigation. The primary particle size of Al_2O_3 is 30 nm, whereas the primary particle size of TiO_2 is 30–50 nm, and both nanoparticles were from Nova Scientific Resources. As base fluid, distilled water and coolant oil are mixed in the proportion of 95:5. This is due to the fact that the one-step technique is better for oxide particles because it increases stability and decreases agglomeration [14]. At first, the Al_2O_3 - TiO_2 hybrid nanofluid was diluted. This was accomplished by dispersing Al_2O_3 and TiO_2 nanoparticles in the base fluid for thirty minutes using the stirring method. The parameters of Al_2O_3 and TiO_2 nanoparticles are summarized in Table 1, with liquid solution with nanoparticles inside and weight concentrations of 20 wt% and 40 wt% for Al_2O_3 and TiO_2 , respectively, as well as the nanoparticle density employed in the formulation and dilution of nano-cutting fluid. The base fluid is a mixture of distilled water and coolant oil (Beiling X-Ten), this mixture was combined using a ratio of 95:5, which is designed for use in cutting fluid applications for CNC machining. The parameters for the base fluid are listed in Table 2. The estimated density of cooling oil is between 700 and 950 kg/m^3 , whereas the density of distilled water is 1000 kg/m^3 .

Table 1. Properties Al_2O_3 - TiO_2 nanoparticles.

Property	Aluminum Oxide	Titanium Oxide
Molecular Formula	Al_2O_3	TiO_2
Form	are liquid	are liquid
Diameter (nm)	30 nm	30–50 nm
Weight concentration (wt%)	20	40
Density (kg/m^3)	4000	4230

Table 2. Properties/information of base fluid.

Property/Information	Coolant Oil	Distilled Water
Density	700–950 kg/m^3	1000 kg/m^3
Type (Brand)	Semi-synthetic(Beiling X-Ten 150)	-
Ratio	5%	95%

As nanoparticles are constantly aggregated due to very strong van der Waals interactions, the production of a homogenous solution remains a technological problem. The development of nano-cutting fluids is impeded by the inadequate characterization of nanoparticle suspensions, which can influence the heat transfer characteristics [15,16]. The tendency of nanofluids with an unstable state to aggregate raises questions regarding their stability. For this reason, the nano-cutting fluid stability test was conducted using four forms of evaluation: Ultraviolet-Visible (UV-Vis) spectrophotometer measurements and analysis, visual observation, TEM analysis, and zeta potential analysis. The UV-Vis analysis was utilized to quantify the time of sonication of nanoparticles suspended in the cutting fluid. The subsequent stage, visual observation of sedimentation, involved

obtaining photos of the sediment for a month. After that, transmission electron microscopy (TEM) investigation was carried out in order to analyze the nanoparticle's size, shape, and dispersion. The stability of hybrid nano-cutting fluids was lastly tested using the zeta potential analysis.

2.2. Workpiece Preparation

Aluminum-based alloys have played a vital role in aerospace manufacturing since the introduction of aircraft with metallic skins. The model was found to accurately represent experimental stress–strain behavior at high temperatures, including strain-rate sensitivity, cyclic softening, ageing effects, transient material behavior, and stress relaxation [17]. Al 7075 is the alloy designation for the workpiece employed in this experiment. Using a roughing carbide insert, the material was prepared prior to the actual machining. Five (5) workpieces of a comparable diameter and length were to be produced using turning methods. A CNC Lathe CT-200 was utilized for the pre-machining procedure. The workpiece's present diameter and length required to be measured first. Next, the procedure of deburring was performed to eliminate any sharp edges. Then, the procedure of facing was utilized to produce a constant length of 305 mm for each workpiece. The turning procedure was also carried out to ensure that each workpiece's diameter was kept at 85.9 mm. The chemical composition and physical parameters of the selected material are depicted in Tables 3 and 4.

Table 3. Chemical composition of Al 7075.

Elements	Max	Min	Actual
Si	0.40	0.00	0.0713
Fe	0.50	0.00	0.1350
Cu	2.00	1.20	1.6100
Mn	0.30	0.00	0.1010
Mg	2.90	2.10	2.3100
Cr	0.28	0.18	0.2360
Zn	6.10	5.10	5.5400
Ti	0.20	0.00	0.0225

Table 4. Mechanical properties of Al 7075.

Test	Ultimate Tensile Strength (UTS)	Yield Tensile Strength (YTS)	Elongation	Hardness
Requirement	≥ 81	≥ 71	≥ 7	
Actual	$89.19/6.15 \times 10^2$	$81.49/5.62 \times 10^2$	10.0	84.7
Unit	ksi/MPa	ksi/MPa	%	HRB

2.3. The Turning Process with MQL-Hybrid Nano-Cutting Fluid

Experiments were primarily focused on the CNC lathe's turning process coupled with the MQL cooling method. Therefore, the machine setup must be dependable so that the MQL system setup does not detach from the tool magazine during the cutting process. Figure 1 depicts the schematic diagram of the MQL turning setup and all the parts or components that are used during the machining process. Figure 2a depicts the CNC lathe (GEIDEMEISTER CT-200) used for the research work. The cross section of the CNC lathe machine with the MQL turning setup installed is shown in Figure 2b. The MQL turning setup was initiated by attaching the MQL cooling system to the tool magazine. Similar procedure was employed by a previous researcher [18]. Prior to carrying out the actual experiment, a trial run with the MQL cooling system was carried out. The setup began when the air compressor inflated the coolant tube by blowing air into the air pressure tube. After which, the hybrid nano-cutting fluid travelled through the tube and MQL nozzle to the cutting tool. The quantity of lubricant that was distributed was regulated by the nozzle.

During the cutting process, the MQL nozzle sprayed nanofluid directly onto the workpiece and tool in the form of a mist. During the cutting process, the cutting temperature was recorded using a temperature gun (Extech IR High Temperature Thermometer 42545, Extech Instruments, Nashua, NH, USA), a reading was taken three times, and the average was calculated. After the cutting process, the surface roughness of the workpiece was measured using a roughness tester (Mitutoyo SJ-210, Mitutoyo, Kawasaki, Japan) that measured roughness in Ra (average roughness) and this considered as a type of contact way to measure a roughness. Then, the weight of the insert was measured before and after the cutting process using a high-accuracy electronic balance (Shimadzu ATX224, Shimadzu, Kyoto, Japan) to assess the tool wear rate.

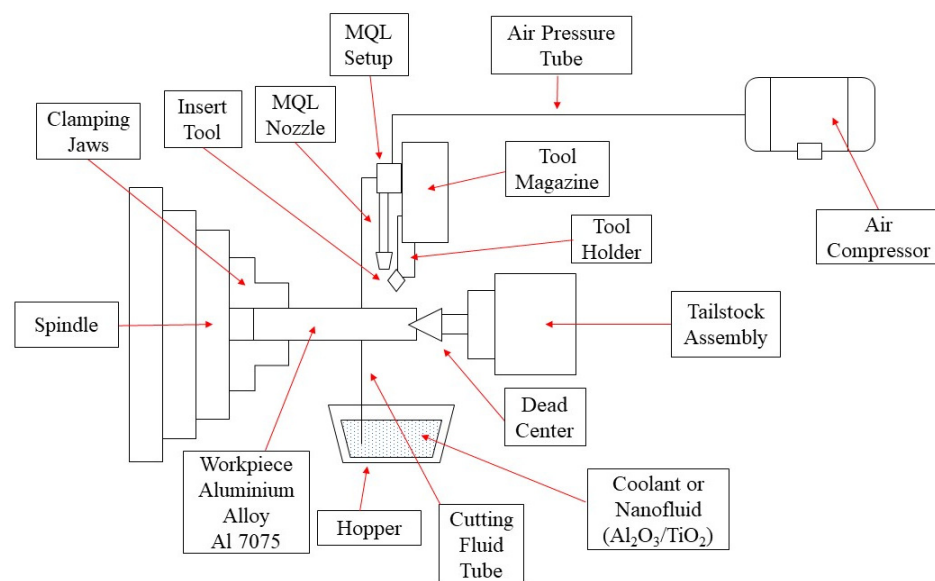


Figure 1. Schematic diagram of MQL turning setup.

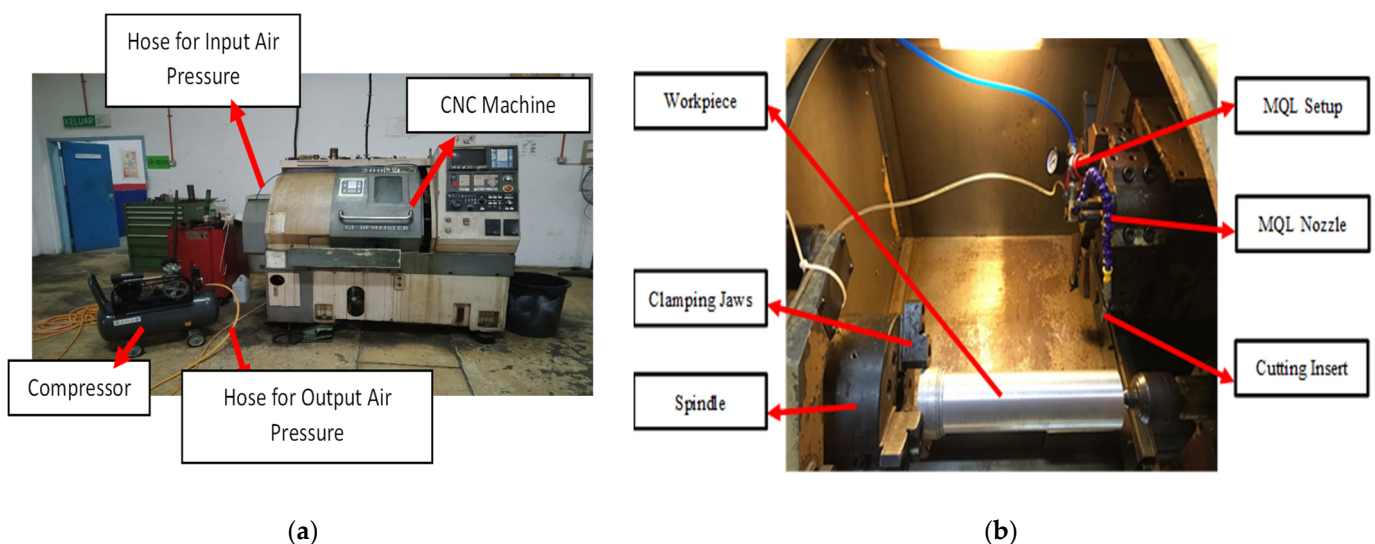


Figure 2. CNC Lathe CT-200. (a) CNC lathe (GEIDEMEISTER CT-200), (b) MQL turning setup.

2.4. Response Surface Method (RSM)

2.4.1. DOE

The DOE utilizing the response method is used to arrange the experiment so that the appropriate number of runs may be determined. Three control factors or input parameters, namely depth of cut (d_o), feed rate (f), and nanoconcentration (ϕ), each with three levels,

were employed in the experiment, and are listed in Table 5. Center composite design (CCD), which focuses on face centered design (FCD), was utilized by the RSM using alpha (α) = 1. Using design expert software, the DOE is calculated and presented in Table 6. Previous studies applied comparable RSM approaches, albeit with different control parameters and values [19]. Using the data selected in Table 5, data collection was performed. Cutting temperature, surface roughness, and tool wear were the responses, or the outcome study. The number of suggested runs by RSM was twenty. The nanoconcentration value was set to 0, 2, and 4%. The value for the depth of cut was set to 0.1 mm, 0.2 mm, and 0.3 mm. Next, feed rates of 0.3 mm/rev, 0.6 mm/rev, and 0.9 mm/rev were set.

Table 5. DOE parameters and levels.

Control Factor	Depth of Cut, Doc (mm)	Feed Rate (mm/rev)	Volume Concentration, ϕ (%)
Level 1	0.3	0.1	0
Level 2	0.6	0.2	2
Level 3	0.9	0.3	4

Table 6. RSM design layout.

Run	ϕ (%)	doc (mm)	F (mm/rev)
1	0.00	0.20	0.60
2	4.00	0.30	0.90
3	2.00	0.20	0.60
4	2.00	0.30	0.60
5	2.00	0.20	0.60
6	2.00	0.10	0.60
7	2.00	0.20	0.30
8	4.00	0.10	0.30
9	2.00	0.20	0.60
10	2.00	0.20	0.60
11	2.00	0.20	0.60
12	0.00	0.10	0.90
13	0.00	0.30	0.90
14	4.00	0.10	0.90
15	0.00	0.10	0.30
16	2.00	0.20	0.90
17	0.00	0.30	0.30
18	2.00	0.20	0.60
19	4.00	0.20	0.60
20	4.00	0.30	0.30

2.4.2. RSM Analysis

To identify the ideal set of input parameters and values that will produce the best possible output performance for these studies, this RSM analysis used the analysis of variance (ANOVA) technique. The ANOVA is a well-known and widely-utilized statistical method for interpreting experimental data by determining the influence ratio of each variable [20]. In addition, the ANOVA is used to determine the importance of each parameter in the context of the overall issue that must be addressed. In addition to this, a regression model was investigated in order to either determine the pattern or determine how the output performance would be affected by higher or lower parameter values.

3. Results and Discussion

This section provides the results as well as a discussion on the stability of nano-cutting fluids, as well as an examination of cutting performance, including cutting temperature, surface roughness, and tool wear.

3.1. The Investigation of Hybrid Nano-Cutting Fluid Stability

3.1.1. Via UV-Vis Spectrophotometer

Figure 3 demonstrates the stability of a 0.001% hybrid nanofluid following preparation for up to 30 days, based on the peak wavelength absorption ratio values. The light absorption values of the five nanofluids vary due to their varying sonication times. The duration of sonication influences the stability of hybrid nanofluids. During the four-week observation period, the light absorption strength decreases significantly. The hybrid nano-cutting fluid with 0 min, 30 min, and 60 min of sonication time exhibited a higher absorption ratio than the fluid with 120 min of sonication time. A nano-cutting fluid that leaves more particle-free zones in the base fluid also results in sediment development and a decrease in fluid stability. At 90 min of sonication, the hybrid nano-cutting fluids exhibited the highest absorption ratio. Therefore, it can be concluded that 90 min of sonication produces the most stable hybrid nano-cutting fluid containing $\text{Al}_2\text{O}_3/\text{TiO}_2$. Therefore, the optimal sonication time is 90 min. Henceforth, all nano-cutting fluids were prepared with a sonication time of 90 min.

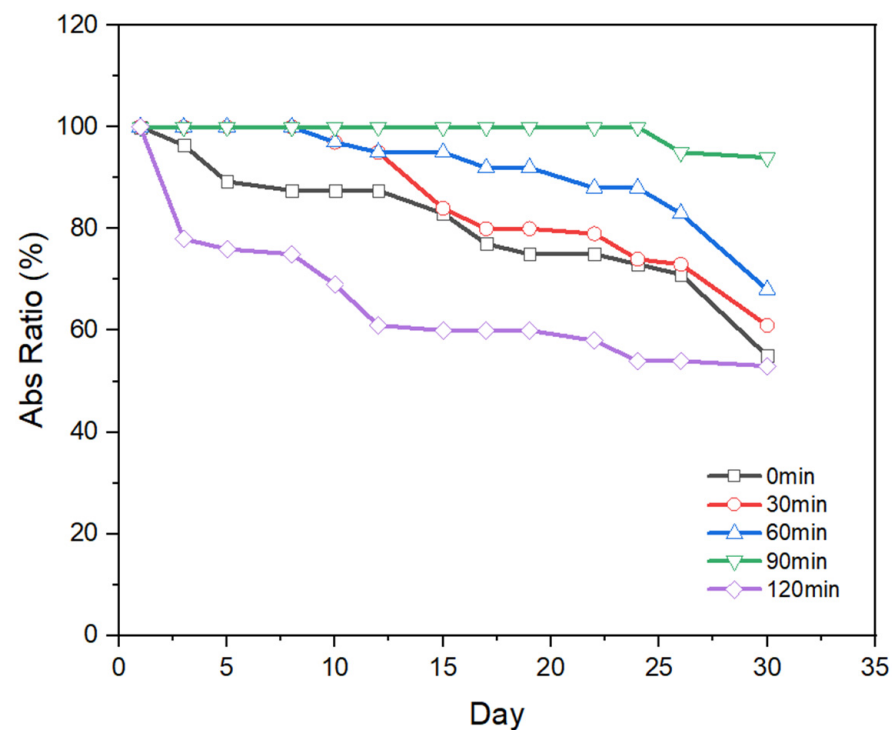


Figure 3. UV-Vis. Spectrum obtained for $\text{Al}_2\text{O}_3\text{-TiO}_2$ hybrid nanofluid for 30 days.

3.1.2. Via Visual Sedimentation

On the first day and 30 days later, images of test tubes containing nanofluid were captured. Figure 4a demonstrates that on the first day, the 1 to 4% hybrid nanofluid does not exhibit any discernible nanoparticle sedimentation. It indicates that the nanofluids are stable immediately after preparation because nanoparticle aggregation has not yet [21]. Figure 4b reveals little sedimentation at the bottom of the test tube and insignificant color separation at the top of the test tube for each of the four hybrid nanofluid samples; thus, it is negligible. When the nanofluids are kept in a static state for four weeks, all of the samples exhibit excellent stability, and the results follow a similar pattern to those of Mukesh Kumar et al. [22].

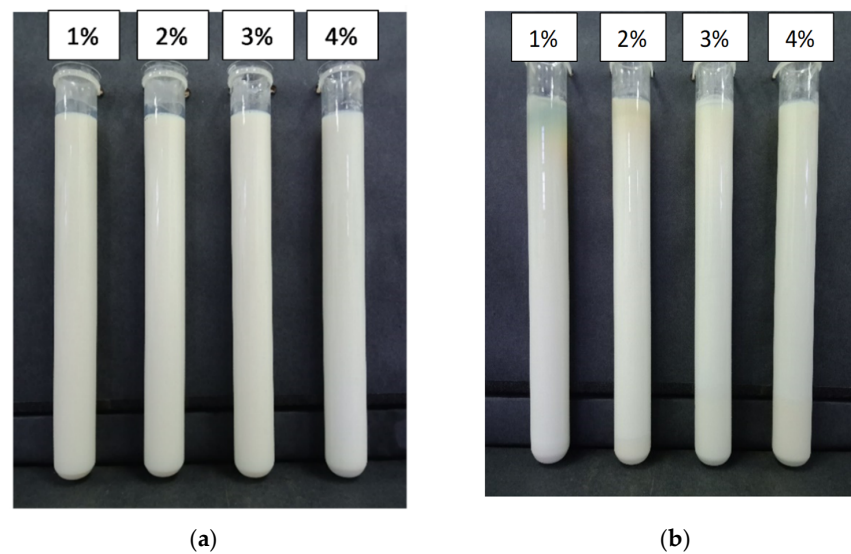


Figure 4. Photograph of $\text{Al}_2\text{O}_3\text{-TiO}_2$ hybrid nanofluid at static condition: (a) just after preparation, (b) after 30 days.

3.1.3. Via Zeta Potential

The zeta potential value of the nanofluid generated for experimental investigation was calculated using Zeta Potential (Anton Paar, Lite Sizer 500, Graz, Austria). The observed Zeta potential value of the synthesized nanofluid is not within the range of the isoelectric point of the $\text{Al}_2\text{O}_3\text{-TiO}_2$ hybrid nanofluid. This measurement error ensures that the nanoparticles in the base fluid are disseminated uniformly and remain stable. Due to extremely high repulsive interactions between nanoparticles, the measured Zeta potential value is outside the range of iso-electric point nanoparticles [23]. The zeta potential for a 0.00001 vol% volume concentration is 37.6 mV. The zeta potential value of the hybrid $\text{Al}_2\text{O}_3\text{-TiO}_2$ nanofluid indicates that the nanofluid concentration has an excellent zeta potential value. With a zeta value of 0.001 vol.% and a volume concentration of 64.2 mV, the nanofluid is extremely stable. Therefore, greater concentration $\text{Al}_2\text{O}_3\text{-TiO}_2$ hybrid nanofluids are more suitable for long-term use than lower concentration nanofluids. Figure 5 compares the current findings to the stability classification proposed by Lee et al. [24].

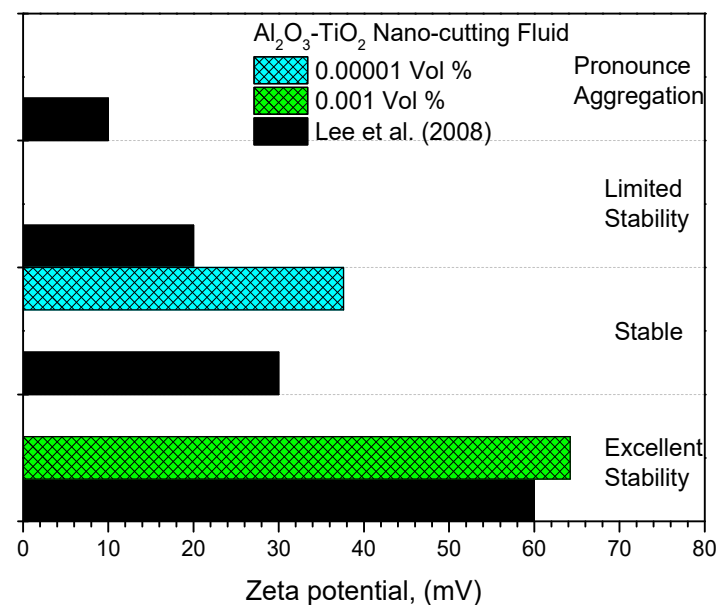


Figure 5. Zeta potential value for different concentration of $\text{Al}_2\text{O}_3\text{-TiO}_2$ hybrid nano-cutting fluids [24].

3.1.4. Via TEM Analysis

TEM analysis confirmed the average size of Al_2O_3 - TiO_2 nanoparticles, as depicted in Figure 6. The Al_2O_3 nanoparticles occupy the space between TiO_2 nanoparticles because Al_2O_3 nanoparticles are larger than TiO_2 nanoparticles. The combination of two nanoparticles of differing sizes would lessen the size difference between smaller and larger particles, hence boosting thermal properties such as dynamic viscosity and heat transfer capacities [25]. In addition, the TEM examination is utilized to observe the dispersion of hybrid nanoparticles in liquid form, thereby validating their stability. The numbers in Figure 6 represent the sizes of adjacent nanoparticles as pointed. The figure also demonstrates that both Al_2O_3 nanoparticles (clearer color) and TiO_2 nanoparticles (darker color) were uniformly disseminated and no significant aggregation had occurred. This is demonstrated in the stability of these hybrid nano-cutting fluids composed of Al_2O_3 and TiO_2 .

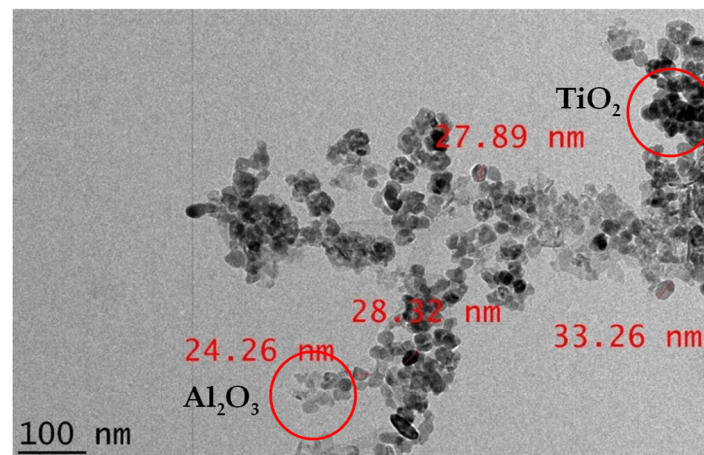


Figure 6. TEM analysis of 28.43 nm average size of Al_2O_3 - TiO_2 nanoparticles.

3.2. Machining with Hybrid Nano-Cutting and MQL

The results of hybrid machining were presented in Table 7, and this machining, which was carried out using combinations of RSM parameters, is comprised of three input parameters and three output responses. Before beginning the cutting process, the combinations of input parameters that were paired with the MQL cooling technique were set at the turning machine.

3.3. Analysis of Cutting Temperature

Table 8 shows the ANOVA analysis for cutting temperature. The results show that the model and the input parameters are significant with values less than 0.05. Further, nanofluid concentration is the most significant factor, with a p -value less than 0.0001 compared to other input parameters. While the lack of fit value is 0.1724, which is not significant as required. Figure 7 shows the effect of nanofluid concentration and feed rate on cutting temperature. The higher the nanoconcentration, the lower the value of cutting temperature. The trend is comparable to Şirin and Kivak [26]. Further, the lower the value of the feed rate, the lower the cutting temperature will be. The lowest reading of cutting temperature is 25.3 °C at a nanofluid concentration of 4%, a feed rate of 0.1 mm/rev, and a 0.55 mm depth of cut, while Viswanathan et al. [27] only obtained 38.1 °C as the lowest cutting temperature when using MQL with conventional coolant, which shows that using a hybrid nano provides significant temperature loss in the cutting zone. Hence, the highest nanofluid concentration and lowest feed rate produce the lowest cutting temperature.

Table 7. Hybrid nano-MQL employed in machining.

Run	Input Parameter			Responses Studied		
	Nano Concentration (%)	Depth of Cut (mm)	Feed Rate (mm/rev)	Cutting Temperature (°C)	Surface Roughness (μm)	Tool Wear (%)
1	0.00	0.20	0.60	33.2	4.726	0.0911
2	4.00	0.30	0.90	27.5	1.799	0.0308
3	2.00	0.20	0.60	28.3	2.841	0.0456
4	2.00	0.30	0.60	30.2	3.687	0.0733
5	2.00	0.20	0.60	28.7	2.953	0.0498
6	2.00	0.10	0.60	27.7	1.958	0.0362
7	2.00	0.20	0.30	28.0	2.195	0.0405
8	4.00	0.10	0.30	25.8	0.494	0.0107
9	2.00	0.20	0.60	28.9	3.206	0.0523
10	2.00	0.20	0.60	29.1	3.326	0.0582
11	2.00	0.20	0.60	29.4	3.794	0.0612
12	0.00	0.10	0.90	32.9	3.816	0.0852
13	0.00	0.30	0.90	34.4	5.316	0.1005
14	4.00	0.10	0.90	26.1	0.517	0.0162
15	0.00	0.10	0.30	32.2	3.705	0.0797
16	2.00	0.20	0.90	29.9	3.619	0.0676
17	0.00	0.30	0.30	33.7	4.854	0.0941
18	2.00	0.20	0.60	29.6	3.591	0.0646
19	4.00	0.20	0.60	26.6	0.795	0.0201
20	4.00	0.30	0.30	27.0	0.851	0.0257

Table 8. ANOVA analysis of cutting temperature.

Source	Sum of Squares	F Value	p-Value	Remarks
Model	124.41	192.62	<0.0001	significant
A- ϕ	111.56	690.89	<0.0001	significant
B- f	6.56	40.63	<0.0001	significant
C-doc	1.68	10.41	0.0056	-
A ²	4.61	28.54	<0.0001	significant
Res.	2.42	-	-	-
LoF	1.30	0.58	0.7825	not significant
Pure Err	1.12	-	-	-
Cor Tot	126.83	-	-	-

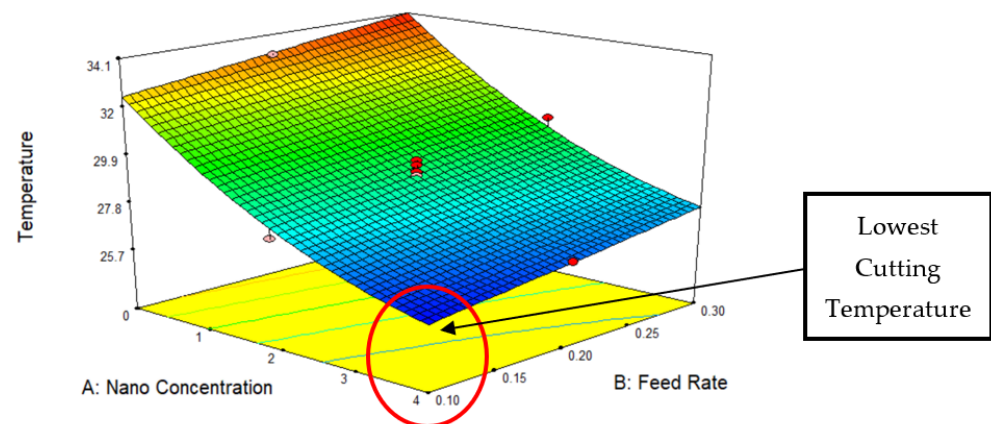


Figure 7. Effect of nanoconcentration (%) and feed rate (mm/rev) on cutting temperature (°C).

3.4. Analysis of Surface Roughness

Table 9 shows the ANOVA analysis for surface roughness. The results show that the model is significant with a value of 0.0001, which is less than 0.05. While the input parameters also have significant values of less than 0.05, the nanoconcentration is the most significant parameter compared to feed rate and depth of cut. With a value of 0.3009 as required, the lack of fit is not significant. Figure 8 depicts the effect of nanofluid concentration and feed rate on the surface roughness. From the graph, it shows a downward trend in the surface roughness value when a higher percentage of nanofluid concentration is used. The pattern is similar to Sinha et al. [28]. A lower feed rate will also result in a better surface finish. The lowest surface roughness of $0.480 \mu\text{m}$ observed when a nanofluid concentration of 4%, a feed rate of 0.1 mm/rev, and a cutting depth of 0.55 mm are used. The lower the surface roughness value (R_a), the smoother the finished surface of the workpiece. However, Viswanathan et al. [27] only obtained $2.734 \mu\text{m}$ as the lowest surface roughness value when using MQL with conventional coolant which indicate that using hybrid nano provides a major roughness deduction on the workpiece surface. Hence, the highest nanofluid concentration, the lowest feed rate, and the lowest depth of cut produce, the best surface finish of the workpiece.

Table 9. ANOVA analysis of surface roughness.

Source	Sum of Squares	F Value	<i>p</i> -Value	Remarks
Model	36.76	63.18	<0.0001	significant
A- ϕ	32.26	166.32	<0.0001	significant
B- f	3.62	18.67	0.0005	significant
C-doc	0.88	4.54	0.0489	significant
Res.	3.10	-	-	-
LoF	2.44	1.66	0.3009	not significant
Pure Err	0.67	-	-	-
Cor Tot	39.86	-	-	-

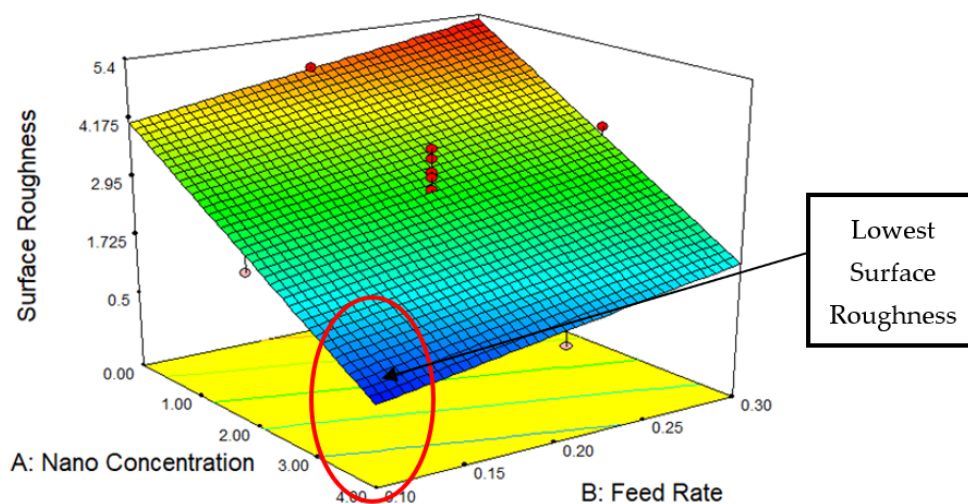


Figure 8. Effect of nanoconcentration (%) and feed rate (mm/rev) on surface roughness (μm).

3.5. Analysis of Tool Wear

Table 10 shows the ANOVA analysis of tool wear. The results show that the model is significant with a *p*-value of less than 0.0001, which is less than 0.05. All the input parameters' *p*-values are less than 0.05, which reflects the significance of all the input. Again, nanoconcentration has the most significant effect of the machining process, and the *p*-value is less than 0.0001. The lack of fit is not significant with the value of 0.7302 as intended. Figure 9 shows the effect of nanofluid concentration and feed rate on tool wear. The higher percentage of nanoconcentration, the lower the value of tool wear. A similar

observation was made by Prasad and Srikant [29]. Further, a lower value of feed rate yield also lowers tool wear. The lower the tool wear value, the longer the tool life of the insert will be. The lowest tool wear value of 0.0104% is achieved when a nanofluid concentration of 4%, a feed rate of 0.1 mm/rev, and a 0.55 mm depth of cut are employed.

Table 10. ANOVA analysis of tool wear.

Source	Sum of Squares	F Value	p-Value	Remarks
Model	0.013	108.23	<0.0001	significant
A- ϕ	0.012	295.83	<0.0001	significant
B-f	9.293×10^{-4}	22.82	0.0002	significant
C-doc	2.460×10^{-4}	6.04	0.0258	significant
Res.	6.516×10^{-4}	-	-	-
LoF	3.886×10^{-4}	0.67	0.7302	not significant
Pure Err	2.630×10^{-4}	-	-	-
Cor Tot	0.014	-	-	-

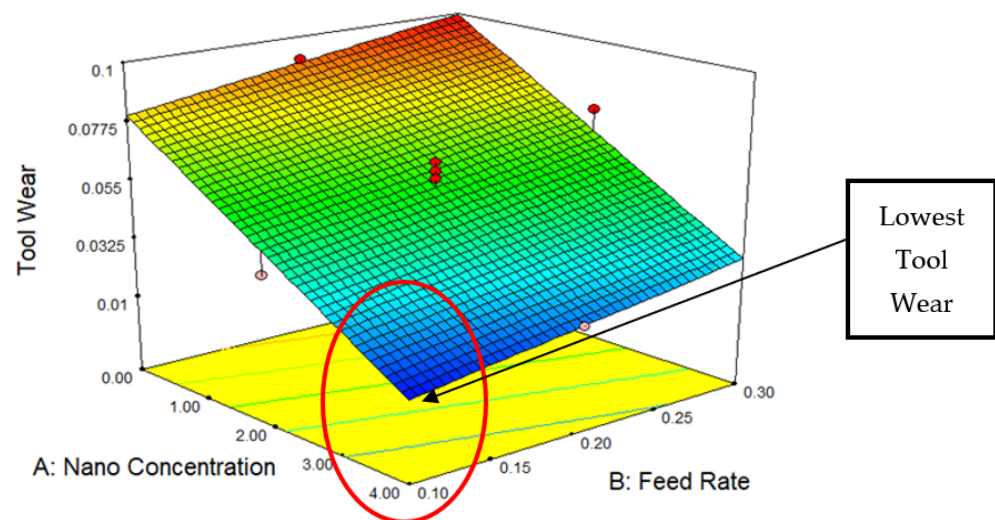


Figure 9. Effect of nanoconcentration (%) and feed rate (mm/rev) on tool wear (%).

3.6. Regression Analysis

The regression analysis or model was utilized to establish the pattern or evaluate the impact of higher or lower parameter values on output performance. The regression analysis was utilized to fit the provided RSM response to a quadratic equation, to investigate the connection between the inputs and outputs of the models, and to ascertain the optimal values for the input parameters [30]. Regression equations 1–3, as follows, indicate the relationship between nanoconcentration, feed rate, and depth of cut in terms of their effects on cutting temperature, surface roughness, and tool wear in the present experiments. As for cutting temperature, surface roughness, and tool wear, these show a similar pattern whereas their value will increase with the combination of nanoconcentration decrease, feed rate increase, and depth of cut increase.

$$\text{Cutting temperature} = 30.84 - 2.63 (\text{nanoconcentration}) + 8.10 (\text{feed rate}) + 1.37 (\text{depth of cut}) + 0.24 (\text{nanoconcentration})^2 \quad (1)$$

$$\text{Surface roughness} = 2.90 - 0.90 (\text{nanoconcentration}) + 6.02 (\text{feed rate}) + 0.99 (\text{depth of cut}) \quad (2)$$

$$\text{Tool wear} = + 0.10 - 0.02(\text{nanoconcentration}) + 0.10 (\text{feed rate}) + 0.02 (\text{depth of cut}) \quad (3)$$

The regression model could predict the correct result within the range of nanoconcentration between 0 and 4%, feed rate of 0.1 to 0.3 mm/rev and depth of cut of 0.3 to 0.9 mm as parameters.

3.7. Optimization and Validations

According to the RSM enhanced-cutting performances, the optimal parameters suggested that the best cutting performances were achieved by combining the lowest depth of cut (0.5 mm), the lowest feed rate (0.1 mm/rev), and the highest volume concentration (4%). The results of validation tests conducted on the specified parameters are presented in Table 11. To test and assess the dependability of the built regression model against the experimental data, optimal-level trial runs were conducted. As can be seen in the table below, the predicted and experimental values are very comparable. Error values for proper statistical analysis must be fewer than 20% [31,32]. All the error values that were assessed were less than 10%, which is acceptable. Consistent with the existing experimental data, the validation results indicated a successful optimization.

Table 11. Ideal parameters and validation.

Cutting Parameters	Nanoconcentration (%)	Feed Rate (mm/rev)	Depth of Cut (mm)
Suggested Parameter	4.0	0.1	0.55
Responses Studied	Cutting Temperature (°C)	Surface Roughness (Ra, μm)	Tool Wear (%)
Prediction Results	25.3	0.480	0.0104
Validation Results	24.9	0.455	0.0094
Percentage Deviation (%)	1.58	5.21	9.62

4. Conclusions

The efficacy of the hybrid Al₂O₃-TiO₂ nano-cutting fluid for the turning process was investigated. Visual sedimentation and the UV-Vis analysis revealed that nano-cutting fluids of varying concentrations were stable for more than a month, while the zeta potential analysis showed beyond-stable conditions for both investigated volume concentrations. The nano-cutting performance of Al₂O₃-TiO₂ hybrid nano-cutting fluid was enhanced through performance investigation using the CNC lathe during the turning process. The nano-cutting fluid with the highest concentration of 4% produced the lowest cutting temperature, surface roughness, and tool wear, resulting in a lower temperature in the cutting zone, a smoother surface, and a longer tool life. The optimal performance parameter for nanofluid concentration was 4%, the feed rate was 0.1 mm/rev, and the depth of cut was 0.55 mm, and these conditions result in the lowest cutting temperature, surface roughness, and tool wear values of 25.3 °C, 0.480 m, and 0.0104%, respectively. It is suggested that future research compares the cooling techniques (flood, dry, and MQL) to demonstrate the superiority of MQL with nanofluid. Investigation on the characteristic analysis involving thermo-properties (thermal conductivity and viscosity) and tribology is necessary to gain a further understanding of the behavior of Al₂O₃-TiO₂ hybrid nano-cutting fluid.

Author Contributions: Conceptualization, A.A. and A.A.M.R.; methodology, A.A. and A.A.M.R.; software, A.A.M.R. and N.N.M.Z.; validation, N.N.M.Z. and W.H.A.; formal analysis, A.A.; investigation, A.A.; resources, A.A., A.A.M.R. and N.N.M.Z.; data curation, A.A. and A.A.M.R.; writing—original draft preparation, A.A. and A.A.M.R.; writing—review and editing, N.N.M.Z. and W.H.A.; visualization, A.A. and A.A.M.R.; supervision, A.A.M.R.; project administration, A.A.M.R. and W.H.A.; funding acquisition, A.A.M.R. All authors have read and agreed to the published version of the manuscript.

Funding: This research was funded by Ministry of Higher Education (MOHE), grant number FRGS/1/2019/TK03/TATI/02/1 and by University College TATI (UCTATI), grant number STG/9001-1902.

Data Availability Statement: The data that support the findings of this study are available from the corresponding author, [W.H. Azmi], upon reasonable request.

Acknowledgments: This research was supported by MOHE through Fundamental Research grant Scheme (FRGS/1/2019/TK03/TATI/02/1). We also want to thank to the University College TATI for the financial support under short term grant (STG/9001-1902).

Conflicts of Interest: No potential conflict of interest was reported by the authors.

Nomenclature

AISI	American Iron and Steel Institute
Al ₂ O ₃	Aluminum Oxide
Al7075	Aluminum 7075
ATX224	An Electronic Balance Model
CCD	Center Composite Design
CNC	Computer Numerical Control
Cr	Chromium
CT-200	Turning Machine Brand
Cu	Copper
doc	depth of cut
DOE	Design of Experiment
Err	Error
f	feedrate
FCD	Face Centered Design
Fe	Iron
H13	chromium-molybdenum hot work steel
HRB	Hardness Rockwell B
IR 42545	A Thermometer Model
kg/m ³	kilogram per meter cube
ksi	kilopound per square inch
LoF	Lack of Fit
Mg	Magnesium
ml	mililiter
mm	milimeter
mm/rev	milimeter per revolution
Mn	Manganese
MPa	Mega Pascal
MQL	Minimum Quantity Lubricant
mV	mili Volt
nm	nanometer
Ra	Arithmetic Average Roughness
Res	Residual
RSM	Response Surface Method
Si	Silicon
SJ-210	A Roughness Tester Model
TEM	Transmission Electron Microscopy
Ti	Titanium
TiO ₂	Titanium Oxide
Tot	Total
UTS	Ultimate Tensile Strength
UV-Vis	Ultra Violet Visible
vol%	volume percentage
wt%	weight percentage
YTS	Yield Tensile Strength
Zn	Zinc
°C	Degree Celcius
%	Percentage
μm	micrometer
φ	nanoconcentration

References

1. Vishnu, A.V.; Kumar, P.J.; Ramana, M.V. Comparison among dry, flooded and MQL conditions in machining of EN 353 steel alloys—an experimental investigation. *Mater. Today Proc.* **2018**, *5*, 24954–24962. [[CrossRef](#)]
2. Khan, N.S.; Shah, Q.; Sohail, A.; Ullah, Z.; Kaewkhao, A.; Kumam, P.; Zubair, S.; Ullah, N.; Thounthong, P. Rotating flow assessment of magnetized mixture fluid suspended with hybrid nanoparticles and chemical reactions of species. *Sci. Rep.* **2021**, *11*, 11277. [[CrossRef](#)] [[PubMed](#)]
3. Debnath, S.; Anwar, M.; Pramanik, A.; Basak, A.K. Nanofluid-Minimum Quantity Lubrication System in Machining: Towards Clean Manufacturing. In *Sustainable Manufacturing*; Elsevier: Amsterdam, The Netherlands, 2021; pp. 109–135.
4. Sharma, A.K.; Tiwari, A.K.; Singh, R.K.; Dixit, A.R. Tribological investigation of TiO₂ nanoparticle based cutting fluid in machining under minimum quantity lubrication (MQL). *Mater. Today Proc.* **2016**, *3*, 2155–2162. [[CrossRef](#)]
5. Shao, Y.; Fergani, O.; Ding, Z.; Li, B.; Liang, S.Y. Experimental investigation of residual stress in minimum quantity lubrication grinding of AISI 1018 steel. *J. Manuf. Sci. Eng.* **2016**, *138*, 011009. [[CrossRef](#)]
6. Mulyadi, I.H.; Balogun, V.A.; Mativenga, P.T. Environmental performance evaluation of different cutting environments when milling H13 tool steel. *J. Clean. Prod.* **2015**, *108*, 110–120. [[CrossRef](#)]
7. Zhang, T.; Zou, Q.; Cheng, Z.; Chen, Z.; Liu, Y.; Jiang, Z. Effect of particle concentration on the stability of water-based SiO₂ nanofluid. *Powder Technol.* **2021**, *379*, 457–465. [[CrossRef](#)]
8. Sharma, A.K.; Singh, R.K.; Dixit, A.R.; Tiwari, A.K. Characterization and experimental investigation of Al₂O₃ nanoparticle based cutting fluid in turning of AISI 1040 steel under minimum quantity lubrication (MQL). *Mater. Today Proc.* **2016**, *3*, 1899–1906. [[CrossRef](#)]
9. Singh, R.K.; Sharma, A.K.; Dixit, A.R.; Tiwari, A.K.; Pramanik, A.; Mandal, A. Performance evaluation of alumina-graphene hybrid nano-cutting fluid in hard turning. *J. Clean. Prod.* **2017**, *162*, 830–845. [[CrossRef](#)]
10. Thakur, A.; Manna, A.; Samir, S. Experimental investigation of nanofluids in minimum quantity lubrication during turning of EN-24 steel. *Proc. Inst. Mech. Eng. Part J J. Eng. Tribol.* **2020**, *234*, 712–729. [[CrossRef](#)]
11. Musavi, S.H.; Davoodi, B.; Niknam, S.A. Effects of reinforced nanoparticles with surfactant on surface quality and chip formation morphology in MQL-turning of superalloys. *J. Manuf. Processes* **2019**, *40*, 128–139. [[CrossRef](#)]
12. Gupta, M.K.; Sood, P.K.; Sharma, V.S. Optimization of machining parameters and cutting fluids during nano-fluid based minimum quantity lubrication turning of titanium alloy by using evolutionary techniques. *J. Clean. Prod.* **2016**, *135*, 1276–1288. [[CrossRef](#)]
13. Zawawi, N.N.M.; Azmi, W.H.; Ghazali, M.F.; Ramadhan, A.I. Performance optimization of automotive air-conditioning system operating with Al₂O₃-SiO₂/PAG composite nanolubricants using Taguchi Method. *Automot. Exp.* **2022**, *5*, 121–136. [[CrossRef](#)]
14. Yu, W.; Xie, H. A review on nanofluids: Preparation, stability mechanisms, and applications. *J. Nanomater.* **2012**, *2012*, 1–17. [[CrossRef](#)]
15. Zawawi, N.N.M.; Azmi, W.H.; Ghazali, M.F. Performance of Al₂O₃-SiO₂/PAG composite nanolubricants in automotive air-conditioning system. *Appl. Therm. Eng.* **2022**, *204*, 117998. [[CrossRef](#)]
16. Zawawi, N.N.M.; Azmi, W.H.; Ghazali, M.F. Tribological performance of Al₂O₃-SiO₂/PAG composite nanolubricants for application in air-conditioning compressor. *Wear* **2022**, *492–493*, 204238. [[CrossRef](#)]
17. Singh, T.; Singh, P.; Dureja, J.; Dogra, M.; Singh, H.; Bhatti, M.S. A review of near dry machining/minimum quantity lubrication machining of difficult to machine alloys. *Int. J. Mach. Mach. Mater.* **2016**, *18*, 213–251. [[CrossRef](#)]
18. Kopac, J. Achievements of sustainable manufacturing by machining. *J. Achiev. Mater. Manuf. Eng.* **2009**, *34*, 180–187.
19. Cetin, M.H.; Kabave Kilincarslan, S. Effects of cutting fluids with nano-silver and borax additives on milling performance of aluminium alloys. *J. Manuf. Processes* **2020**, *50*, 170–182. [[CrossRef](#)]
20. Faheem, A.; Husain, T.; Hasan, F.; Murtaza, Q. Effect of nanoparticles in cutting fluid for structural machining of Inconel 718. *Adv. Mater. Process. Technol.* **2020**, *8*, 259–276. [[CrossRef](#)]
21. Abdullah, M.I.H.C.; Othman, A.; Abdullah, R.; Abdollah, M.F. Optimization on the nanoparticles stability in liquid phased condition by using Taguchi analysis. *J. Adv. Res. Fluid Mech. Therm. Sci.* **2019**, *61*, 129–139.
22. Mukesh Kumar, P.C.; Palanisamy, K.; Vijayan, V. Stability analysis of heat transfer hybrid/water nanofluids. *Mater. Today Proc.* **2020**, *21*, 708–712. [[CrossRef](#)]
23. Mahbulbul, I.M. Stability and Dispersion Characterization of Nanofluid. In *Preparation, Characterization, Properties and Application of Nanofluid*; William Andrew Publishing: Gazipur, Bangladesh, 2019; pp. 47–112. [[CrossRef](#)]
24. Lee, J.H.; Hwang, K.S.; Jang, S.P.; Lee, B.H.; Kim, J.H.; Choi, S.U.S.; Choi, C.J. Effective viscosities and thermal conductivities of aqueous nanofluids containing low volume concentrations of Al₂O₃ nanoparticles. *Int. J. Heat Mass Transf.* **2008**, *51*, 2651–2656. [[CrossRef](#)]
25. Sharif, S.; Sadiq, I.O.; Yusof, N.M.; Mohruni, A.S. A review of minimum quantity lubrication technique with nanofluids application in metal cutting operations. *Int. J. Adv. Sci. Eng. Inf. Technol.* **2017**, *7*, 587–593. [[CrossRef](#)]
26. Şirin, Ş.; Kivak, T. Performances of different eco-friendly nanofluid lubricants in the milling of Inconel X-750 superalloy. *Tribol. Int.* **2019**, *137*, 180–192. [[CrossRef](#)]
27. Viswanathan, R.; Ramesh, S.; Subburam, V. Measurement and optimization of performance characteristics in turning of Mg alloy under dry and MQL conditions. *Measurement* **2018**, *120*, 107–113. [[CrossRef](#)]
28. Sinha, M.K.; Madarkar, R.; Ghosh, S.; Rao, P.V. Application of eco-friendly nanofluids during grinding of Inconel 718 through small quantity lubrication. *J. Clean. Prod.* **2017**, *141*, 1359–1375. [[CrossRef](#)]

29. Prasad, M.M.S.; Srikant, R.R. Performance evaluation of nano graphite inclusions in cutting fluids with MQL technique in turning of AISI 1040 steel. *Int. J. Res. Eng. Technol.* **2013**, *2*, 381–393.
30. Sarfraz, M.H.; Jahanzaib, M.; Ahmed, W.; Hussain, S. Multi-response parametric optimization of squeeze casting process for fabricating Al 6061-SiC composite. *Int. J. Adv. Manuf. Technol.* **2019**, *102*, 759–773. [[CrossRef](#)]
31. Derdour, F.Z.; Kezzar, M.; Khochemane, L. Optimization of penetration rate in rotary percussive drilling using two techniques: Taguchi analysis and response surface methodology (RSM). *Powder Technol.* **2018**, *339*, 846–853. [[CrossRef](#)]
32. Cetin, M.H.; Ozcelik, B.; Kuram, E.; Demirbas, E. Evaluation of vegetable based cutting fluids with extreme pressure and cutting parameters in turning of AISI 304L by Taguchi method. *J. Clean. Prod.* **2011**, *19*, 2049–2056. [[CrossRef](#)]